
This is an electronic reprint of the original article.
This reprint may differ from the original in pagination and typographic detail.

Wang, Weijun; Andric, Nikola; Sarch, Cody; Silva, Bruno T.; Tenkanen, Maija; Master, Emma R.

Constructing arabinofuranosidases for dual arabinoxylan debranching activity

Published in:
Biotechnology and Bioengineering

DOI:
[10.1002/bit.26445](https://doi.org/10.1002/bit.26445)

Published: 01/01/2018

Document Version
Publisher's PDF, also known as Version of record

Published under the following license:
Unspecified

Please cite the original version:
Wang, W., Andric, N., Sarch, C., Silva, B. T., Tenkanen, M., & Master, E. R. (2018). Constructing arabinofuranosidases for dual arabinoxylan debranching activity. *Biotechnology and Bioengineering*, 115(1), 41-49. <https://doi.org/10.1002/bit.26445>

This material is protected by copyright and other intellectual property rights, and duplication or sale of all or part of any of the repository collections is not permitted, except that material may be duplicated by you for your research use or educational purposes in electronic or print form. You must obtain permission for any other use. Electronic or print copies may not be offered, whether for sale or otherwise to anyone who is not an authorised user.

ARTICLE

Constructing arabinofuranosidases for dual arabinoxylan debranching activity

Weijun Wang¹  | Nikola Andric¹ | Cody Sarch¹ | Bruno T. Silva¹ |
Maija Tenkanen² | Emma R. Master^{1,3}

¹Department of Chemical Engineering and Applied Chemistry, University of Toronto, Toronto, Ontario, Canada

²Department of Food and Environmental Sciences, University of Helsinki, Helsinki, Finland

³Department of Bioproducts and Biosystems, Aalto University, Espoo, Finland

Correspondence

Weijun Wang, Department of Chemical Engineering and Applied Chemistry, University of Toronto, 200 College Street, Toronto, Ontario, M5S 3E5, Canada.
Email: wce.wang@utoronto.ca

Funding information

ERC Consolidator Grant to EM (BHIVE), Grant number: 648925; The Natural Sciences and Engineering Research Council of Canada for the Strategic Network Grant "Industrial Biocatalysis Network"; Forest FAB: Applied Genomics for Functionalized Fibre and Biochemicals, Grant number: ORF-RE-05-005; Jenny and Antti Wihuri Foundation to MT

Abstract

Enzymatic conversion of arabinoxylan requires α -L-arabinofuranosidases able to remove α -L-arabinofuranosyl residues (α -L-Araf) from both mono- and double-substituted D-xylopyranosyl residues (Xylp) in xylan (i.e., AXH-m and AXH-d activity). Herein, SthAbf62A (a family GH62 α -L-arabinofuranosidase with AXH-m activity) and BadAbf43A (a family GH43 α -L-arabinofuranosidase with AXH-d3 activity), were fused to create SthAbf62A_BadAbf43A and BadAbf43A_SthAbf62A. Both fusion enzymes displayed dual AXH-m,d and synergistic activity toward native, highly branched wheat arabinoxylan (WAX). When using a customized arabinoxylan substrate comprising mainly α -(1 \rightarrow 3)-L-Araf and α -(1 \rightarrow 2)-L-Araf substituents attached to disubstituted Xylp (d-2,3-WAX), the specific activity of the fusion enzymes was twice that of enzymes added as separate proteins. Moreover, the SthAbf62A_BadAbf43A fusion removed 83% of all α -L-Araf from WAX after a 20 hr treatment. ¹H NMR analyses further revealed differences in SthAbf62A_BadAbf43 rate of removal of specific α -L-Araf substituents from WAX, where 9.4 times higher activity was observed toward d- α -(1 \rightarrow 3)-L-Araf compared to m- α -(1 \rightarrow 3)-L-Araf positions.

KEYWORDS

α -L-arabinofuranohydrolase, activity synergy, arabinoxylan fusion enzyme, dual α -L-Araf debranching activity

1 | INTRODUCTION

As the second most abundant plant cell wall polysaccharide after cellulose, xylan is a suitable feedstock for the production of fuels, chemicals, nutraceuticals, and materials (Deutschmann & Dekker, 2012; Gírio et al., 2010; Sedlmeyer, 2011). Xylan consists of a linear β -(1 \rightarrow 4)-linked D-xylopyranosyl (β -D-Xylp) backbone, which depending on the source, can be partially substituted at O-2 positions and/or O-3 positions with α -L-arabinofuranosyl (α -L-Araf) residues and acetyl groups, and at O-2 positions with α -D-glucopyranosyluronic acid (GlcP) or 4-O-methyl GlcP (MeGlcP) residues (Aspinall, 1980;

Dumon, Song, Bozonnet, Fauré, & O'Donohue, 2012; Scheller & Ulvskov, 2010). The O-5 position of some α -L-Araf residues can be further esterified with *p*-coumaric or ferulic acid (Saulnier, Vigouroux, & Thibault, 1995; Scheller & Ulvskov, 2010). The branching chemistry of xylan significantly impacts its solubility and adherence to other biopolymers (Bosmans et al., 2014).

(Methyl)-Glucuronoxylan is the predominant form of xylan in deciduous dicots (i.e., angiosperms including hardwood trees). By contrast, xylan from conifers (i.e., gymnosperms including softwood trees) and lignified tissues of monocots (e.g., grasses and cereal husks) contain both (Me)GlcP and α -L-Araf substituents with varying

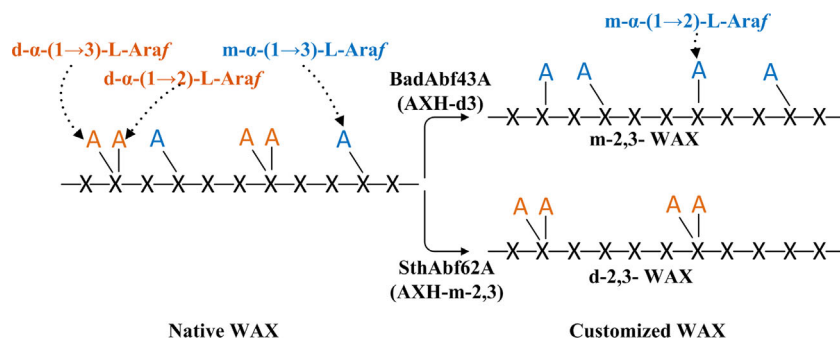


FIGURE 1 Schematic structures of native and customized wheat arabinoxylan used in this study. A: L-Araf; X: D-Xylp. AXH-m and AXH-m-2,3 represent activity measurements on m-2,3-WAX, whereas AXH-d represents activity toward d-2,3-WAX. AXH-m,d activity indicates that the enzyme acts on both m-2,3-WAX, and d-2,3-WAX, as well as, native WAX

contents, whereas xylan in cereal endosperm is mainly arabinoxylan (Figure 1) (Deutschmann & Dekker, 2012; Girio et al., 2010; Lu, Walker, Muir, Mascara, & O'Dea, 2000; Mikkonen & Tenkanen, 2012; Scheller & Ulvskov, 2010). L-Araf residues are also found in other plant cell wall polysaccharides, including arabinan, pectin, arabinogalactan and others, representing the second most abundant pentose in plant species after D-xylose (Seiboth & Metz, 2011). Consistent with the molecular diversity of xylans, its complete enzymatic hydrolysis typically requires the concerted action of several enzymes, including endo- β -1,4-xylanases, and β -xylosidases that target glycosidic linkages within the xylan backbone, along with α -L-arabinofuranosidases, α -glucuronidases, acetyl xylan esterases, feruloyl esterases, as well as, glucuronoyl esterases, which target branching substituents present in different xylan structures (Biely, Singh, & Puchart 2016; Coughlan & Hazlewood, 1993; Gilbert, Stålbrand, & Brumer, 2008; Shallom & Shoham, 2003).

α -L-Arabinofuranosidases (EC 3.2.1.55) have been classified into several carbohydrate-active enzyme (CAZy) families (www.cazy.org), including GH1, GH3, GH43, GH51, GH54, GH62, and GH93. Arabinoxylan arabinofuranohydrolase (AXH) corresponds to those α -L-arabinofuranosidases displaying L-arabinose debranching activity toward polymeric arabinoxylan, and have the potential to fine tune xylan chemistry or facilitate complete xylan hydrolysis (Deutschmann & Dekker, 2012; Heikkinen et al., 2013; O'Donohue & Hahn-Hägerdal, 2012; Pitkänen, Tuomainen, Virkki, & Tenkanen, 2011). Family GH62 α -arabinofuranosidases and several specific GH43 α -arabinofuranosidases characterized to date display AXH activity, and strict substrate specificity toward (1 \rightarrow 2)-and/or (1 \rightarrow 3)-linked α -L-Araf from mono-substituted Xylp residues (i.e., m- α -(1 \rightarrow 2)-L-Araf, m- α -(1 \rightarrow 3)-L-Araf substituents). The resulting AXH-m,2,3 activity has been rationalized by the narrow and deep active site pocket (-1 subsite) for m- α -L-Araf residue binding and cleavage observed in corresponding enzyme structures (Kaur et al., 2014; Maehara et al., 2014; Siguier et al., 2014; Wang et al., 2014). On the other hand, family GH43 α -L-arabinofuranosidases from *Bifidobacterium adolescentis* (BadAbf43A), *Humicola insolens* (HiAXHd3), and *Chrysosporium lucknowense* C1(Abn7) were found to exclusively cleave α -(1 \rightarrow 3)-L-Araf residues linked to disubstituted Xylp (i.e., d- α -(1 \rightarrow 3)-L-Araf substituents) (Pouvreau, Joosten, Hinz, Gruppen, & Schols, 2011;

Sørensen et al., 2006; Van Laere, Beldman, & Voragen, 1997). In the case of HiAXHd3, AXH-d3 activity was explained by a comparatively shallow L-arabinose binding cleft adjacent to a deep active site pocket (McKee et al., 2012). Determinants of AXH-d3 regio-selectivity, however, remain unclear. Finally, a few studies have reported GH51 and GH54 enzymes with AXH-m, d type activity toward the non-reducing end terminal Xylp; however, AXH-m, d type activity toward internal Araf disubstitutions in polymeric arabinoxylans was comparatively weak (Ferré, Broberg, Duus, & Thomsen, 2000; Koutaniemi & Tenkanen, 2016; Sakamoto, Inui, Yasui, Hosokawa, & Ihara, 2013).

Applications of arabinoxylans are expected to benefit from the discovery and development of α -arabinofuranosidases able to efficiently remove α -L-Araf from both singly and doubly substituted Xylp residues (i.e., AXH-m,d activity). Herein, we present our efforts to create α -L-arabinofuranosidases for debranching m,d- α -L-Araf from arabinoxylan. First, a structure-guided, site-specific mutagenesis approach was applied in an effort to confer AXH-m,d activity to the GH62 α -L-arabinofuranosidase from *Streptomyces thermoviolaceus*, SthAbf62A. While the predicted significance of the R239 in SthAbf62A was experimentally confirmed, gain in AXH-d activity for SthAbf62A was not achieved. A protein fusion comprising SthAbf62A and BadAbf43A, however, led to a functional enzyme with AXH-m,d activity toward native wheat arabinoxylan (WAX), which surpassed the activity of enzymes combined as single proteins.

2 | MATERIALS AND METHODS

2.1 | Chemicals

KAPA HiFi HotStart ReadyMix was purchased from Kapa Biosystems (Wilmington, MA). Wheat arabinoxylan (WAX, high viscosity, purity: ~95%, contains 18% m- α -L-Araf, 18% d- α -L-Araf, and 59% xylose, Ara:Xyl = 0.61) (Pitkänen et al., 2011), endo-1,4- β -xylanase from *Neocallimastix patriciarum* and α -L-arabinofuranosidase from *Bifidobacterium* sp (E-AFAM2, AXH-d3) were purchased from Megazyme (Wicklow, Ireland). Genomic DNA from *Bifidobacterium adolescentis* (strain ATCC 15703) was purchased from the American Type Culture Collection (ATCC).

All other chemicals were analytical grade and were obtained from Sigma-Aldrich (Oakville, ON, Canada) or Fisher Scientific (Ottawa, ON, Canada).

2.2 | DNA manipulation

The gene encoding the mature form of BadAbf43A (Genbank ID: AY233379 from 1167 to 2756) was amplified using the forward and reverse primers P1 and P2 shown in supplementary Table S1. PCR was performed using the KAPA HiFi HotStart ReadyMix and the following 30 × PCR cycles: denaturation at 98°C for 20 s, primer annealing at 55°C for 20 s and elongation at 72°C for 90 s. The infusion cloning kit from Clontech (Mountain View, CA) was used to transfer purified PCR products to expression vector p15Tv-L (GenBank accession EF456736), generating p15Tv-L_BadAbf43A. Site-specific mutagenesis of SthAbf62A was carried out according to a modified Quik-Change™ (Stratagene, Santa Clara, CA) method that uses partially overlapping primers (Supplemental Table S1) (33). All constructs were verified by sequencing at the Center of Applied Genomics in SickKids Hospital in Toronto, Canada.

2.3 | Design and construction of fusion enzymes

Overlap extension PCR was used to fuse *SthAbf62A* and *BadAbf43A* genes in both orientations (Horton, Hunt, Ho, Pullen, & Pease, 1989). Briefly, the coding sequence for *BadAbf43A* and *SthAbf62A* were amplified from p15Tv-L_BadAbf43A and p15Tv-L_SthAbf62A using the primer pairs of P3/P4 and P5/P6 (Supplemental Table S1), respectively. The resulting PCR products were combined such that the matching sequences at their 3' ends would overlap and act as primers for elongation to generate fusion gene *BadAbf43A_SthAbf62A*. The PCR product was purified by 1% agarose gel and then transferred to into p15Tv-L by using the infusion cloning kit from Clontech. Similarly, primer pairs of P7/P8 and P9/P10 were used for *SthAbf62A_BadAbf43A* construction.

2.4 | Production and purification of enzymes

E. coli BL21 (λDE3) codon plus harboring the plasmid with each target gene was propagated in 1 L of Luria-Bertani medium supplemented with 0.5 M d-sorbitol, 2.5 mM glycine betaine, 34 μg/ml chloramphenicol, and 100 μg/ml ampicillin at 37°C. When an optical density of 0.6 was reached at 600 nm wavelength, isopropyl β-d-thiogalactopyranoside was added to induce protein expression in a final concentration of 0.5 mM. The culture was incubated at 15°C overnight and then harvested by centrifugation at 6,000g for 20 min.

The cell pellet was suspended in binding buffer (300 mM NaCl, 50 mM HEPES, pH 7.0, 5% Glycerol, 5 mM imidazole) and disrupted by sonication. The cell debris was removed by centrifugation (17,500g, 20 min). The clear supernatant was incubated with Ni-NTA resin (Ni²⁺-nitrilotriacetate, Qiagen, Toronto, ON, Canada) for 45 min at 4°C. The resin was then washed with 200 ml of washing buffer (300 mM NaCl, 50 mM HEPES, pH 7.0, 5% (v/v) glycerol,

50 mM imidazole) and eluted with ~30 ml of elution buffer (300 mM NaCl, 50 mM HEPES, pH 7.0, 5% v/v glycerol, 250 mM imidazole). Active fractions were pooled, desalted with Bio-Gel® P10 and loaded onto Uno-Q chromatography column (5.0 ml) and eluted with a 20-column volume linear gradient of 0–500 mM NaCl. Chromatography was performed on a BIOSHOP Duoflow (Bio-Rad, Mississauga, ON, Canada). Centrifugal Filter Units (10 K; Millipore, Etobicoke, ON, Canada) were used for concentrating protein and transferring the purified protein to 25 mM HEPES buffer (pH 7.0). Protein aliquots were flash frozen in liquid nitrogen and then stored at –80°C.

Protein concentrations were determined using the Bradford assay (Bradford, 1976) and Bio-Rad reagents (Bio-Rad, Canada); bovine serum albumin was used as a standard. SDS-PAGE was performed and stained with Coomassie Blue R-250 and according to established procedures (Laemmli, 1970). The Pageruler Plus Prestained Protein Ladder (10–170 kDa, Fermentas) was used to estimate protein molecular size.

2.5 | Preparation of WAX with only single or double α-l-Araf substitutions

Arabinoxylan having mainly (1 → 2) and (1 → 3) linked α-l-Araf monosubstituents (m-2, 3-WAX) (Figure 1) was generated through enzymatic removal of d-α-(1 → 3)-l-Araf from doubly substituted Xylp using a commercial α-l-arabinofuranosidase from *Bifidobacterium* sp (AXH-d3, E-AFAM2 from Megazyme) as described previously (Sakamoto et al., 2011; Wang et al., 2014).

Doubly substituted arabinoxylan (d-2,3-WAX) was generated by using SthAraf62A to remove m-α-l-Araf residues (Figure 1). Briefly, in a 50 ml reaction comprising 100 mM HEPES buffer (pH 7.0), 10.0 mg/ml of WAX was treated with 2.1 mg of the SthAraf62A at 45°C for 24 hr. An additional 1.05 mg of SthAraf62A was then added and the reaction was incubated for an additional 24 hr to maximize m-α-l-Araf removal from arabinoxylan. The precipitated arabinoxylan resulting from m-α-l-Araf debranching was removed by centrifugation (15,000g, 20 min). SthAraf62A was inactivated by adding 4.2 ml 2.0 M NaOH to the supernatant and incubating at 70°C for 10 min. The reaction was then neutralized by adding 4.2 ml 2.0 M HCl. Doubly substituted arabinoxylan in supernatant was then recovered using 95% ethanol and then freeze dried as described previously (Wang et al., 2014).

2.6 | Enzyme activity assays

Activity toward various arabinoxylans (i.e., WAX, m-2,3-WAX, and d-2,3-WAX) was monitored using the Nelson-Somogyi assay for reducing sugars release (Smogyi, 1952). The standard assay solution contained 5.0 mg/mL arabinoxylan in 0.2 ml of 100 mM HEPES buffer (pH 7.0). The reaction was initiated by adding an amount of enzyme determined to release products in a linear relation to time when incubated at 40°C for 20 min. One unit of the activity was defined as the amount of enzyme releasing 1 μmol of L-(+)-arabinose equivalent per minute. L-(+)-Arabinose (Sigma-Aldrich) was used to generate a standard curve (0.05–0.6 mg/ml). All enzyme assays were carried out in triplicate.

2.7 | Optimum reaction pH and enzyme thermostability

All the enzyme assays were performed using the standard aforementioned activity assay with native WAX as substrate. The effect of pH on enzyme activity was determined by performing the activity assay at pH range from 3.5 to 10.5 with increments of 0.5 pH units; a universal buffer (100 mM acetic acid, 100 mM boric acid, and 100 mM phosphoric acid, adjusted to the target pH using sodium hydroxide solution) was used for this analysis. The thermostability of fusion enzyme was evaluated by incubating the enzyme at 25–80°C for 60 min in 100 mM HEPES buffer (pH 7.0) before measuring residual enzyme activity.

2.8 | ^1H NMR analysis for monitoring L-Araf removal by fusion enzyme from arabinoxylan

To quantitatively evaluate the regio-selectivity and debranching rate of the generated fusion enzymes on native WAX, one-dimensional ^1H NMR spectra were collected for the treated arabinoxylan with different reaction time (Wang et al., 2014). Briefly, 10.0 mg/ml native WAX was treated with 610 μg of SthAraf62A_BadAbf43A in a 10.0 ml reaction solution containing 100 mM HEPES buffer (pH 7.0) at 40°C. At regular time intervals (12 time points over 20 hr), 0.6 ml aliquots were transferred from the reaction to 0.05 ml 2.0 M NaOH, heat-treated at 70°C for 10 min to ensure inactivation of the enzyme, and then neutralized using 0.05 ml of 2.0 M HCl. The treated arabinoxylan was then precipitated by adding 1.3 ml of 95% ethanol and separated by centrifugation (15,000g, 10 min). The pellet was suspended in 0.6 ml water and again precipitated with 1.3 ml 95% ethanol. The resulting arabinoxylan was digested using GH11 β -1,4-endoxylanase from *Neocallimastix patriciarum* (Megazyme), and corresponding ^1H NMR spectra were obtained and processed as previously described (Wang et al., 2014). The region between 5.48–5.39 ppm corresponds to m- α -L-(1 \rightarrow 3) Araf substituents and that of 5.29–5.23 ppm corresponds to d- α -L-(1 \rightarrow 2) Araf substituents (Wang et al., 2014). However, a decrease in peak area within the 5.29–5.23 ppm region can represent a depletion in d- α -L-(1 \rightarrow 3) Araf substituents, given the resulting signal shift from 5.29–5.23 ppm to 5.29–5.37 ppm when d- α -L-(1 \rightarrow 2) Araf becomes m- α -L-(1 \rightarrow 2) Araf. Finally, the region between 5.37–5.29 ppm is the combined signal of d- α -L-(1 \rightarrow 3) Araf and m- α -L-(1 \rightarrow 2) Araf. Therefore, a decrease in this signal can only represent net m- α -L-(1 \rightarrow 2) Araf removal since release of d- α -L-(1 \rightarrow 3) Araf would be compensated by corresponding m- α -L-(1 \rightarrow 2) Araf formation. Taking this information into account, residual α -Araf in WAX was calculated as follows:

Equation 1:

$$\% \text{ of residual } \alpha\text{-L-Araf in WAX} = \frac{\text{Peak area of selected ppm region after enzyme treatment}}{\text{Peak area of selected ppm region before enzyme treatment}} \times 100 \quad (1)$$

The total m,d- α -L-Araf removal from WAX was calculated using the change in peak area corresponding to the 5.48–5.23 ppm region.

3 | RESULTS AND DISCUSSION

3.1 | Structure-guided site-specific mutagenesis of SthAbf62A

SthAbf62A is a thermostable GH62 family α -arabinofuranosidase from *Streptomyces thermoviolaceus* displaying AXH-m-2,3 activity (Wang et al., 2014). Previous structural analysis of SthAbf62A revealed a narrow substrate binding pocket to accommodate a m- α -L-Araf substituent, flanked by a binding cleft that presumably accommodates the xylan backbone structure. Close inspection of the protein structure complexed with xylo-tetraose (PDB ID: 4O8P) predicted a spatial clash between d- α -L-Araf substituents, and the side chain of the highly conserved arginine 239 (R239) residue (numbering based on PDB ID: 4O8N). Accordingly, in an effort to gain dual AXH-m,d activity, R239 in SthAbf62A was replaced by an alanine to reduce the size of the functional R-group. Its surrounding residues, including F212 and I233, were also mutated to alanine in an effort to further expand α -L-Araf binding pocket (Figure 2). Whereas I233 is not highly conserved, F212 was generally conserved across the GH62 family with exceptions being substitutions to W or L residues.

Compared to the wild-type enzyme, variants R239A, R239K, and R239S exhibited between 30 and 150 times lower specific activity toward native WAX and customized m-2,3-WAX, whereas the specific activity of variants R239A/F212A and R239A/I233A was reduced by between 300 and 500 times (Table 1). The specific activity of the triple mutant (R239A/F212A/I233A) was even further

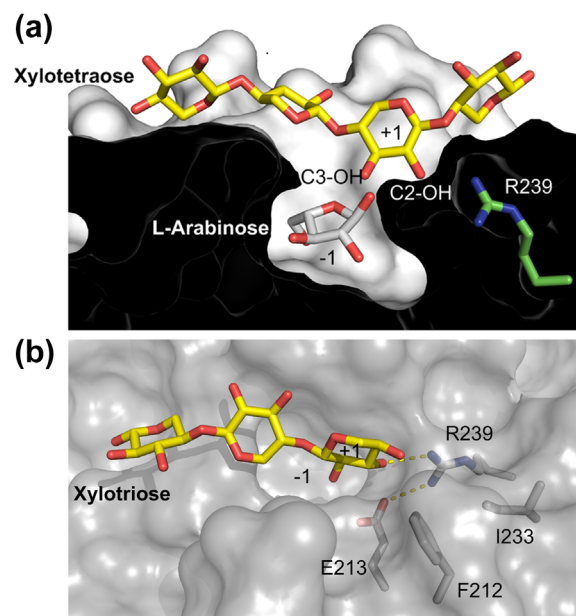


FIGURE 2 Amino acid residues in SthAbf62A selected for site-specific mutagenesis. (a) The narrow arabinose binding pocket along with the xylan backbone binding cleft. The arginine residue of R239 will cause a steric hindrance for d- α -L-Araf substituents accommodation. (b) R239 is shown along with residues of F212 and I233A. The R239 formed an ion pair with catalytic residue E213 and a hydrogen bond with C3-OH in Xylp

TABLE 1 Specific activity of SthAbf62A and its mutants toward arabinoxylan with different arabinose substitutions

Enzymes	Specific activity ^a (mmol product/min/mmol enzyme)		
	Native WAX	m-2, 3-WAX	d-2, 3-WAX ^b
Wild type	320.4 ± 27.9	236.3 ± 8.7	Not detected
R239A	3.0 ± 0.5	7.7 ± 0.7	Not detected
R239K	3.2 ± 0.1	7.1 ± 0.1	Not detected
R239S	2.1 ± 0.3	1.8 ± 0.3	Not detected
R239A/F212A	1.6 ± 0.1	0.9 ± 0.1	Not detected
R239A/I233A	1.3 ± 0.2	0.8 ± 0.2	Not detected
R239A/F212A/ I233A	0.04 ± 0.004	0.06 ± 0.002	Not detected

^aThe final substrate concentration was 5 mg/ml (w/v); products formed by wild-type SthAbf62A were measured after 20 min at 40°C, whereas reactions using mutant enzymes proceeded for 20 hr. *n* = 3; errors indicate standard deviation.

^bNo activity was observed on d-2,3-WAX after 20 hr at 40°C.

impacted, and had decreased by 3,900–8,000 times relative to the wild type enzyme. Moreover, AXH-d activity was not detected after the 20 hr treatment with any of the variants generated using doubly substituted arabinoxylan (d-2,3-WAX) (Table 1). Still, the detrimental impacts of R239 mutagenesis on specific activity revealed its important role in catalysis. The similar activity measured for R239K and R239A variants was initially surprising as both lysine and arginine are expected to be positively charged at the reaction pH (7.0). However, the guanidinium group in arginine allows interactions through its three asymmetrical nitrogen atoms (N^ε, N^{η1}, N^{η2}) compared to only one nitrogen atom (N^δ) in lysine. Furthermore, the structure of the SthAbf62A-xylofuranose complex (PDB ID: 4O8P) predicts an ion pairing between N^{η1} in R239 and O^{ε2} in E213 with a distance of 3.0 Å, as well as a hydrogen bond between N^{η2} in R239 and C3-OH in Xylp (subsite + 1) from xylofuranose (orientation 2) with a distance of 2.9 Å (Figure 2b) (Wang et al., 2014). Altogether, the current mutagenesis study implies that R239 may play a role in positioning and deprotonating the catalytic residue E213 through ionic interactions, as well as anchoring Xylp unit (subsite + 1) through hydrogen bonding.

3.2 | Benefit of protein fusion to protein production

Prediction of AXH-m, d activity based on sequence and structure remains a challenging task. Instead, the fusion of SthAbf62A and BadAbf43A is an alternative route to create a single enzyme with dual AXH-m,d activity (Figure 3a), showing potential benefits over application of separate enzymes in terms of protein production and synergistic action.

Herein, SthAbf62A_BadAbf43A and BadAbf43A_SthAbf62A were successfully constructed without adding an additional linker sequence, as the structure of SthAbf62A and the BadAbf43A homologue (HiAXH-d3) displayed flexible loop regions in both N- and C-termini (McKee et al., 2012; Wang et al., 2014), which were predicted to impart flexibility to the connected enzymes. Notably, several previous fusion enzymes were also developed without

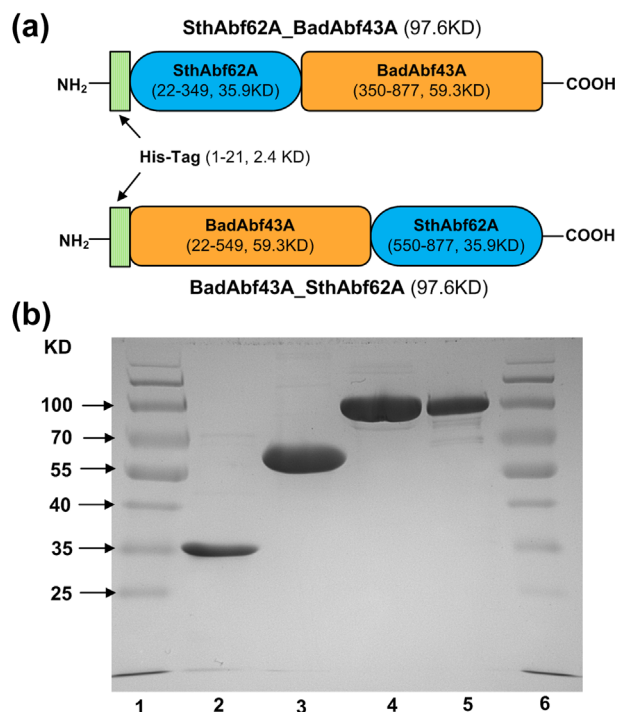


FIGURE 3 Design and SDS-PAGE analysis of the fusion constructs. (a) Construction of fusion α -L-arabinofuranosidases by linking SthAbf62A with BadAbf43A in both orientations. (b) SDS-PAGE analysis of enzymes produced and used in this study. Lanes 1, 6: Molecular weight standards; lane 2: SthAbf62A; lane 3: recombinant BadAbf43A; lane 4: SthAbf62A_BadAbf43A fusion enzyme; lane 5: BadAbf43A_SthAbf62A fusion enzyme

additional linker sequences (Rizk, Antranikian, & Elleuche, 2012). The fusion enzymes were overexpressed and purified to homogeneity (Figure 3). The electrophoretic molecular weight of the fusion enzymes was approximately 100 KDa, consistent with the calculated molecular weight of the proteins (97641.21 Da) (Figure 3b). Of note, the yield of SthAbf62A_BadAbf43A after purification was 0.4 μ mol/L culture, which is similar to the yield of SthAbf62A (0.34 μ mol/L) and BadAbf43A (0.4 μ mol enzyme/L) (Supplemental Table S3). As SthAbf62A and BadAbf43A activities were retained in the fusion construct (see below), fusion of the enzymes to generate SthAbf62A_BadAbf43A led to overall gains in yield of recombinant enzyme activity. Notably, the BadAbf43A_SthAbf62A fusion was less stable, where partial proteolysis within the flexible loop region between two parent enzymes resulted in two protein bands (Supplemental Figure S2), and lower final purification yield of the fusion construct (Supplemental Table S3).

3.3 | General properties of the fusion enzymes displaying AXH-m, d activity

Both fusion enzymes released m,d- α -L-Araf substituents from WAX (Table 2), thus representing a first engineered α -arabinofuranosidase with dual AXH-m,d activity. The pH optimum of SthAbf62A_BadAbf43A was 7.0, which was slightly higher than that of BadAbf43A_SthAbf62A at pH 6.5, but still within the range of the parent

enzymes [pH 6.5–7.5 for BadAbf43A (Van Laere et al., 1997); pH 7.0 for SthAbf62A (Wang et al., 2014)] (Figure 4a). SthAbf62A_BadAbf43A retained 40% activity after 1 hr of incubation at 55°C, whereas SthAbf62A and BadAbf43A retained 73% and 0.03% activity, respectively, under the same conditions (Figure 4b). Like BadAbf43A, BadAbf43A_SthAbf62A also lost all detectable activity after 1 hr of incubation at 55°C (Figure 4b), further exemplifying the impact of domain organization on the overall stability of the fusion construct. The effect of domain swapping on enzyme properties was also found for the fusion enzymes of xylanase and glucanase (Liu et al., 2012).

3.4 | Dual AXH-m, d activity and synergistic action of the fusion constructs

As previously reported, SthAbf62A displayed a strict selectivity toward α -(1 \rightarrow 2) and α -(1 \rightarrow 3) linked α -L-Araf units to mono-substituted Xylp residues (Wang et al., 2014); however, its activity on m-2,3-WAX was 26% lower than that on native WAX (Table 2). In m-2, 3-WAX, both α -L-Araf positions would constitute targets for the hydrolysis by SthAbf62A, whereas in native WAX, only the preferred m-(1 \rightarrow 3)- α -L-Araf substituent would be available (Wang et al., 2014). It is conceivable then, that lower activity of SthAbf62A toward m-2,3-WAX compared to native WAX reflects the higher rate of SthAbf62A action toward m-(1 \rightarrow 3)- α -L-Araf substituents over m-(1 \rightarrow 2)- α -L-Araf substituents. Consistent with earlier reports (Van Laere et al., 1997), the recombinant BadAbf43A prepared in this study targeted native WAX and d-2,3-WAX but not m-2, 3-WAX (Table 2), confirming its exclusive action on d- α -(1 \rightarrow 3)-L-Araf positions. Moreover, the specific activity of BadAbf43A toward d-2, 3-WAX was 35% higher than that on WAX (Table 2). One

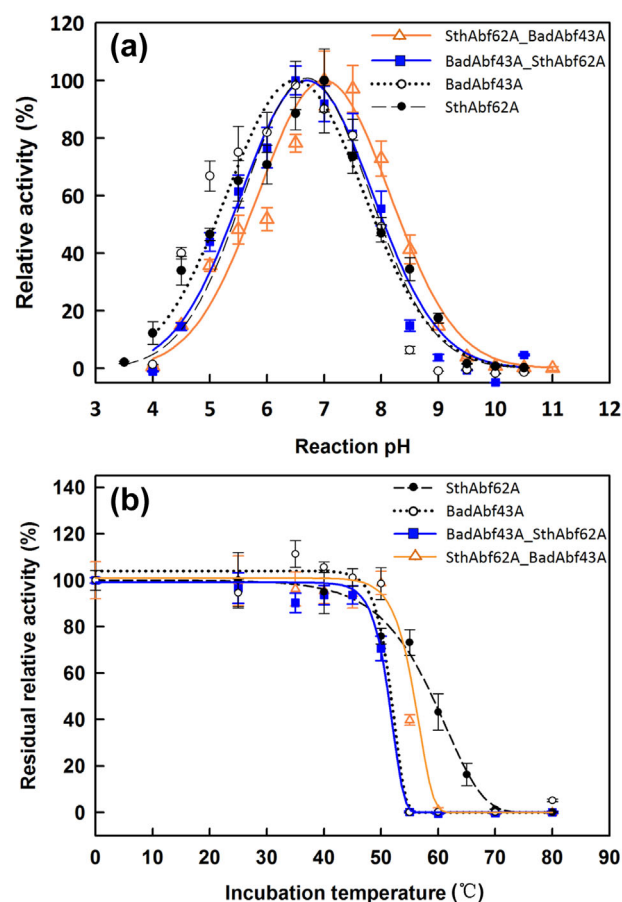


FIGURE 4 General biochemical properties of fusion and parent enzymes. (a) pH-activity profiles; (b) thermostability profiles. Activity assays were performed using 0.5% (w/v) WAX and 0.4 μ g enzymes in 200 μ l of 100 mM HEPES buffer (pH 7.0)

TABLE 2 The dual and synergistic action of constructed fusion enzymes on native and customized wheat arabinoxylans

Enzyme	Specific activity ^a (mmol product/min/mmol enzyme)		
	Native wheat arabinoxylan (WAX)	Mono-2,3-arabinoxylan (m-2,3-WAX)	Di-2,3-arabinoxylan (d-2,3-WAX)
SthAbf62A	320.4 \pm 27.9	236.3 \pm 8.7	Not detected ^b
BadAbf43A	538.3 \pm 25.9 ^c	NO	727.3 \pm 84.8
Sum of the parent activities ^c	858.7 (100%)	236.3 (100%)	727.3 (100%)
SthAbf62A + BadAbf43A ^c	860.3 \pm 91.2 (100.1%)	211.7 \pm 17.2 (89.6%)	898.1 \pm 39.4 (123.5%)
SthAbf62A_BadAbf43A	1117.9 \pm 103.5* (130.1%)	189.3 \pm 10.9 (80.1%)	1467.8 \pm 71.6** (201.8%)
BadAbf43A_SthAbf62A	1240.5 \pm 28.1** (144.5%)	141.9 \pm 6.1** (60.1%)	1531.9 \pm 53.6** (210.6%)

^aTo permit comparison of separate, combined, and fused enzymes, the dose of each enzyme in a 200 μ l reaction was set to 0.025 nmol (i.e., 0.025 nmol of each SthAbf62A and BadAbf43A when applied separately and alone or in combinations, and 0.025 nmol of the SthAbf62A-BadAbf43A or BadAbf43A-SthAbf62A fusion construct). The final substrate concentration was 5.0 mg/ml. Values in brackets represent relative activity, where the sum of parent enzyme activities represents 100%.

^bNo activity was observed on d-2, 3-WAX after 20 hr at 40°C.

^cThe activity of the recombinant BadAbf43A toward native WAX was approximately 50% lower than that reported for the commercial enzyme preparation (Megazyme: E-AFAM2, AXH-d3, 1200 mmol product/min/mmol). This difference likely reflects differences in substrate concentration used to measure enzyme activity (1% WAX for E-AFAM2, 0.5% WAX for the recombinant BadAbf43A) and differences in the reaction pH (pH 6.0 for E-AFAM2, optimum pH (pH 7.0) for the recombinant BadAbf43A). $n = 3$; errors indicate standard deviation.

*Indicates significant difference from enzymes added separately (SthAbf62A + BadAbf43A), $p < 0.05$.

**Indicates significant difference from enzymes added separately (SthAbf62A + BadAbf43A), $p < 0.01$.

explanation for the observed result might be the steric hindrance imposed by $m\text{-}\alpha\text{-(1}\rightarrow\text{3)-L-Araf}$ substituents.

At least two bacterial α -arabinofuranosidases annotated in the in CAZy database comprise both GH62_1 and GH43 domains (i.e., ACB76517 and AJQ96215); however, no functional characterization has been performed for these proteins. Both fusion enzymes constructed herein uniquely displayed α -L-Araf debranching activity toward $m\text{-2,3-WAX}$, $d\text{-2,3-WAX}$, as well as the native WAX (Table 2). Moreover, synergistic action of the fusion constructs was measured on native WAX, where $\text{BadAbf43A_SthAbf62A}$ and $\text{SthAbf62A_BadAbf43A}$ showed 130–145% activity, respectively, relative to the sum of activities of the parent enzymes ($p < 0.05$) (Table 2). Synergistic activities were even greater (over 200%, $p < 0.01$) when using $d\text{-2,3-WAX}$ as the substrate. By comparison, the relative activities of equimolar mixtures of separate enzymes were approximately 100% and 124% (Table 2). The measured benefit of enzyme fusion could be explained by increased proximity of corresponding active sites, such that the product of BadAbf43A is immediately available to SthAbf62A ; alternatively, SthAbf62A may alleviate potential steric hindrance presented by $m\text{-}\alpha\text{-(1}\rightarrow\text{3)-L-Araf}$ substituents. Notably, compared to the parent enzymes, activities of the fusion constructs on $m\text{-2,3-WAX}$

decreased by 10–30%. This could again reflect negative impact of mono-substituted Xylp positions on the activity of the fusion constructs, in this case possibly through non-productive binding of the BadAbf43A component to $m\text{-}\alpha\text{-L-Araf}$ residues.

3.5 | Parallel and sequential debranching of WAX by $\text{SthAbf62A_BadAbf43A}$

Considering enzyme stability and yield, $\text{SthAbf62A_BadAbf43A}$ demonstrated better overall performance as compared to $\text{BadAbf43A_SthAbf62A}$. $\text{SthAbf62A_BadAbf43A}$ activity was thus further analyzed using $^1\text{H-NMR}$ to evaluate its preference toward specific Araf substituents in native WAX substrate. Consistent with the respective specific activities of parent enzymes (Table 2), $\text{SthAbf62A_BadAbf43A}$ revealed approximately 9.4 times faster release of $d\text{-}\alpha\text{-(1}\rightarrow\text{3)-L-Araf}$ substituents compared to $m\text{-}\alpha\text{-(1}\rightarrow\text{3)-L-Araf}$ positions, where the initial removal rates were 1433 ± 276 and $152 \pm 14 \mu\text{mol L-arabinose} \cdot \text{min}^{-1} \cdot \mu\text{mol}^{-1}$ enzyme, respectively (Figure 5). Lowest rates of removal were observed for $m\text{-}\alpha\text{-(1}\rightarrow\text{2)-L-Araf}$ positions, and were also preceded by a lag phase consistent with the initial release of the neighbouring $d\text{-}\alpha\text{-(1}\rightarrow\text{3)-L-Araf}$ substituent (Figure 5b).

Release of L-Araf from WAX by $\text{SthAbf62A_BadAbf43A}$ promoted the formation of xylan aggregates; a similar affect was observed using an equimolar mixture of the parent enzymes. Corresponding $^1\text{H-NMR}$ analyses showed that 83.3% L-Araf substituents had been released from native WAX after 20 hr of $\text{SthAbf62A_BadAbf43A}$ treatment, which was consistent with the L-arabinose yield of $3.59 \pm 0.27 \text{ mg}$ from 10.0 mg WAX (Megazyme, high viscosity) in 1.0 ml reaction solution (L-arabinose recovery rate: $88.7 \pm 7.5\%$) measured using the reducing sugar method.

4 | CONCLUSION

Structure guided site-specific mutagenesis of SthAbf62A was performed to identify residues that restrict enzyme action toward di-substituted Xylp residues of arabinoxylan. While this approach did not yield an enzyme variant with dual, AXH-m, d activity, the analysis revealed the importance of the R239 residue in catalysis. Instead, the fusion enzymes $\text{SthAbf62A_BadAbf43A}$ and $\text{BadAbf43A_SthAbf62A}$ were functionally expressed and showed dual and synergistic AXH-m,d activity toward native WAX and customized $d\text{-2,3-WAX}$. $^1\text{H NMR}$ analysis of $\text{SthAbf62A_BadAbf43A}$ action showed differences in rates of $\alpha\text{-(1}\rightarrow\text{3)-L-Araf}$ versus $\alpha\text{-(1}\rightarrow\text{2)-L-Araf}$ removal, consistent with the specific activities of the parent enzymes. Our work highlights the practicality of protein fusion when the objective is gain, rather than change, in enzyme function. Moreover, the increase in specific activity of $\text{SthAbf62A_BadAbf43A}$ compared to the parent enzymes, together with the ability to double the enzyme activity recovered from a given cultivation, highlights the applied significance of the fusion construct, and potential advantages of analogous constructs for enzymes acting on polymers with varying substituents.

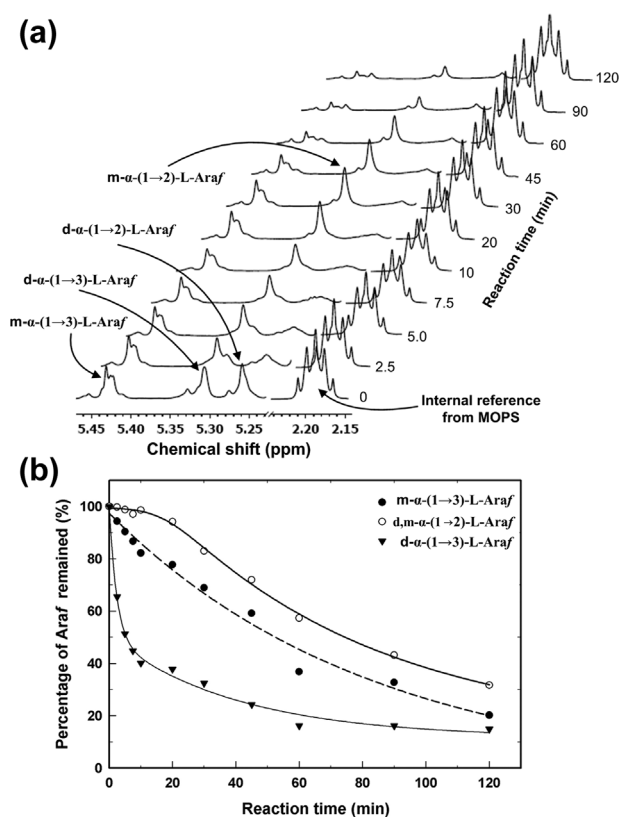


FIGURE 5 $^1\text{H-NMR}$ analysis of reaction products. (a) $^1\text{H-NMR}$ spectra tracking $\alpha\text{-L-Araf}$ removal from WAX over 2 hr. (b) Percentage of remaining $\alpha\text{-L-Araf}$ in WAX at regular time intervals up to 2 hr. The reaction was performed at 40°C and comprised $610 \mu\text{g}$ $\text{SthAbf62A_BadAbf43A}$ and 1% (w/v) WAX in 10 ml 100 mM HEPES buffer (pH 7.0). The region between 5.37–5.29 ppm is the combined signal of $d\text{-}\alpha\text{-(1}\rightarrow\text{3)-L-Araf}$ and $m\text{-}\alpha\text{-(1}\rightarrow\text{2)-L-Araf}$

ACKNOWLEDGMENTS

This work was funded by the Government of Ontario for the project "Forest FAB: Applied Genomics for Functionalized Fibre and Biochemicals" (ORF-RE-05-005), the Natural Sciences and Engineering Research Council of Canada for the Strategic Network Grant "Industrial Biocatalysis Network," and an ERC Consolidator Grant to EM (BHIVE-648925). MT thanks Jenny and Antti Wihuri Foundation for funding the research sabbatical period. All authors reviewed the results and approved the final version of the manuscript. We thank Dr. Peter J. Stogios for the insightful discussion.

ORCID

Weijun Wang  <http://orcid.org/0000-0001-9283-5619>

REFERENCES

- Aspinall, G. O. (1980). Chemistry of cell wall polysaccharides. In J. Preiss (Ed), *The biochemistry of plants, vol 3. Carbohydrates: Structure and function* (pp. 477–500). New York, NY: Academic Press.
- Biely, P., Singh, S., & Puchart, V. (2016). Toward enzymatic breakdown of complex plant xylan structures: State of the art. *Biotechnology Advances*, 34, 1260–1274.
- Bosmans, T. J., Stépán, A. M., Toriz, G., Rennekar, S., Karabulut, E., Wågberg, L., & Gatenholm, P. (2014). Assembly of debranched xylan from solution and on nanocellulosic surfaces. *Biomacromolecules*, 15, 924–930.
- Bradford, M. M. (1976). A rapid and sensitive method for the quantitation of microgram quantities of protein utilizing the principle of protein-dye binding. *Analytical Biochemistry*, 72, 248–254.
- Coughlan, M. P., & Hazlewood, G. P. (1993). Beta-1,4-D-xylan-degrading enzyme systems: biochemistry, molecular biology and applications. *Biotechnology Applied Biochemistry*, 17, 259–289.
- Deutschmann, R., & Dekker, R. F. H. (2012). From plant biomass to bio-based chemicals: Latest developments in xylan research. *Biotechnology Advances*, 30, 1627–1640.
- Dumon, C., Song, L., Bozonnet, S., Fauré, R., & O'Donohue, M. J. (2012). Progress and future prospects for pentose-specific biocatalysts in biorefining. *Process Biochemistry*, 47, 346–357.
- Ferré, H., Broberg, A., Duus, J. O., & Thomsen, K. K. (2000). A novel type of arabinoxylan arabinofuranohydrolase isolated from germinated barley analysis of substrate preference and specificity by nano-probe NMR. *European Journal of Biochemistry*, 267, 6633–6641.
- Gilbert, H. J., Stålbrand, H., & Brumer, H. (2008). How the walls come crumbling down: Recent structural biochemistry of plant polysaccharide degradation. *Current Opinion in Plant Biology*, 11, 338–348.
- Girio, F. M., Fonseca, C., Carvalho, F., Duarte, L. C., Marques, S., & Bogel-Łukasik, R. (2010). Hemicelluloses for fuel ethanol: A review. *Bioresource Technology*, 101, 4775–4800.
- Heikkinen, S. L., Mikkonen, K. S., Pirkkalainen, K., Serimaa, R., Joly, C., & Tenkanen, M. (2013). Specific enzymatic tailoring of wheat arabinoxylan reveals the role of substitution on xylan film properties. *Carbohydrate Polymers*, 92, 733–740.
- Horton, R. M., Hunt, H. D., Ho, S. N., Pullen, J. K., & Pease, L. R. (1989). Engineering hybrid genes without the use of restriction enzymes: Gene splicing by overlap extension. *Gene*, 77, 61–68.
- Kaur, A. P., Nocek, B. P., Xu, X., Lowden, M. J., Leyva, J. F., Stogios, P. J., ... Savchenko, A. (2014). Functional and structural diversity in GH62 α -L-arabinofuranosidases from the thermophilic fungus *Scytalidium thermophilum*. *Microbial Biotechnology*, 8, 419–433.
- Koutaniemi, S., & Tenkanen, M. (2016). Action of three GH51 and one GH54 α -arabinofuranosidases on internally and terminally located arabinofuranosyl branches. *Journal of Biotechnology*, 229, 22–30.
- Laemmli, U. K. (1970). Cleavage of structural proteins during the assembly of the head of bacteriophage T4. *Nature*, 227, 680–685.
- Liu, L., Wang, L., Zhang, Z., Guo, X., Li, X., & Chen, H. (2012). Domain-swapping of mesophilic xylanase with hyper-thermophilic glucanase. *BMC Biotechnology*, 12, 28.
- Lu, Z. X., Walker, K. Z., Muir, J. G., Mascara, T., & O'Dea, K. (2000). Arabinoxylan fiber, a byproduct of wheat flour processing, reduces the postprandial glucose response in normoglycemic subjects. *American Journal of Clinical Nutrition*, 71, 1123–1128.
- Maehara, T., Fujimoto, Z., Ichinose, H., Michikawa, M., Harazono, K., & Kaneko, S. (2014). Crystal structure and characterization of the glycoside hydrolase family 62 α -L-arabinofuranosidase from *Streptomyces coelicolor*. *The Journal of Biological Chemistry*, 289, 7962–7972.
- LS McKee, MJ Pena, A. Rogowski, A. Jackson, RJ Lewis, WS York, ... J Marles-Wright. Introducing endo-xylanase activity into an exo-acting arabinofuranosidase that targets side chains. *Proceedings of the National Academy of Sciences* 109 2012; 6537–6542
- Mikkonen, K. S., & Tenkanen, M. (2012). Sustainable food-packaging materials based on future biorefinery products: Xylans and mannans. *Trends in Food Science and Technology*, 28, 90–102.
- O'Donohue, M. J., & Hahn-Hägerdal, B. (2012). Biomass-derived pentoses. *Process Biochemistry*, 47, 345.
- Pitkänen, L., Tuomainen, P., Virkki, L., & Tenkanen, M. (2011). Molecular characterization and solution properties of enzymatically tailored arabinoxylans. *International Journal of Biological Macromolecules*, 49, 963–969.
- Pouvreau, L., Joosten, R., Hinz, S. W., Gruppen, H., & Schols, H. A. (2011). *Chrysosporium lucknowense* C1 arabinofuranosidases are selective in releasing arabinose from either single or double substituted xylose residues in arabinoxylans. *Enzyme and Microbial Technology*, 48, 397–403.
- Rizk, M., Antranikian, G., & Elleuche, S. (2012). End-to-end gene fusions and their impact on the production of multifunctional biomass degrading enzymes. *Biochemical and Biophysical Research Communications*, 428, 1–5. <http://www.ncbi.nlm.nih.gov/pubmed/23058915>
- Sakamoto, T., Inui, M., Yasui, K., Hosokawa, S., & Ihara, H. (2013). Substrate specificity and gene expression of two *Penicillium chrysogenum* α -L-arabinofuranosidases (AFQ1 and AFS1) belonging to glycoside hydrolase families 51 and 54. *Applied Microbiology and Biotechnology*, 97, 1121–1130.
- Sakamoto, T., Ogura, A., Inui, M., Tokuda, S., Hosokawa, S., Ihara, H., & Kasai, N. (2011). Identification of a GH62 α -L-arabinofuranosidase specific for arabinoxylan produced by *Penicillium chrysogenum*. *Applied Microbiology and Biotechnology*, 90, 137–146.
- Saulnier, L., Vigouroux, J., & Thibault, J. F. (1995). Isolation and partial characterization of feruloylated oligosaccharides from maize bran. *Carbohydrate Research*, 272, 241–253.
- Scheller, H. V., & Ulvskov, P. (2010). Hemicelluloses. *Annual Review of Plant Biology*, 61, 263–289.
- Sedlmeyer, F. B. (2011). Xylan as by-product of biorefineries: Characteristics and potential use for food applications. *Food Hydrocolloids*, 25, 1891–1898.
- Seiboth, B., & Metz, B. (2011). Fungal arabinan and L-arabinose metabolism. *Applied Microbiology and Biotechnology*, 89, 1665–1673.
- Shallom, D., & Shoham, Y. (2003). Microbial hemicellulases. *Current Opinion in Microbiology*, 6, 219–228.
- Siguier, B., Haon, M., Nahoum, V., Marcellin, M., Burlet-Schiltz, O., Coutinho, P. M., & Henrissat, B. (2014). First structural insights into α -L-arabinofuranosidases from the two GH62 glycoside hydrolase subfamilies. *The Journal of Biological Chemistry*, 289, 5261–573.
- Smogyi, M. (1952). Notes on sugar determination. *The Journal of Biological Chemistry*, 195, 19–23.

- Sørensen, H. R., Jørgensen, C. T., Hansen, C. H., Jørgensen, C. I., Pedersen, S., & Meyer, A. S. (2006). A novel GH43 α -L-arabinofuranosidase from *Humicola insolens*: Mode of action and synergy with GH51 α -L-arabinofuranosidases on wheat arabinoxylan. *Applied Microbiology and Biotechnology*, 73, 850–861.
- Van Laere, K. M. J., Beldman, G., & Voragen, G. J. (1997). A new arabinofuranohydrolase from *Bifidobacterium adolescentis* able to remove arabinosyl residues from double-substituted xylose units in arabinoxylan. *Applied Microbiology and Biotechnology*, 47, 231–235.
- Wang, W., Mai-Gisoni, G., Stogios, P. J., Kaur, A., Xu, X., Cui, H., . . . Master, E. R. (2014). Elucidation of the molecular basis for arabinoxylan-Debranching activity of a thermostable family GH62 α -L-Arabinofuranosidase from *Streptomyces thermoviolaceus*. *Applied and Environmental Microbiology*, 80, 5317–5329.

SUPPORTING INFORMATION

Additional Supporting Information may be found online in the supporting information tab for this article.

How to cite this article: Wang W, Andric N, Sarch C, Silva BT, Tenkanen M, Master ER. Constructing arabinofuranosidases for dual arabinoxylan debranching activity. *Biotechnology and Bioengineering*. 2018;115:41–49. <https://doi.org/10.1002/bit.26445>